JOURNAL OF Applied Polymer SCIENCE

Effects of the Extractant on the Hydrophilicity and Performance of High-Density Polyethylene/Polyethylene-*b*-Poly(ethylene glycol) Blend Membranes Prepared via a Thermally Induced Phase Separation Process

Jun-Li Shi, Li-Feng Fang, Hong Zhang, Zhi-Ying Liang, Bao-Ku Zhu, Li-Ping Zhu
Department of Polymer Science and Engineering, Key Laboratory of Macromolecule Synthesis and Functionalization, Ministry of Education, Zhejiang University, Hangzhou 310027, People's Republic of China
Correspondence to: B.-K. Zhu (E-mail: zhubk@zju.edu.cn)

ABSTRACT: The blending of a block copolymer into the membrane matrix is a convenient and efficient way to modify membranes. In this study, high-density polyethylene/polyethylene-*b*-poly(ethylene glycol) (PEG) membranes were prepared via a thermally induced phase separation process, and the extractant effect was investigated. An interesting finding was that the nonpolar extractant (*n*-hexane) was more conducive to the surface enrichment of the PEG chains than the polar solvent (ethanol). The reason was deemed to be the combined effect of the entropy drive, interfacial energy, and swelling behavior. In addition, the membrane performance related to the surface chemical properties was studied. The results suggest that the prepared blend membranes extracted by *n*-hexane showed enhanced the hydrophilicity, antifouling properties, and water flux. © 2013 Wiley Periodicals, Inc. J. Appl. Polym. Sci. 130: 3816–3824, 2013

KEYWORDS: blends; hydrophilic polymers; membranes; polyolefins; surfaces and interfaces

Received 3 January 2013; accepted 17 April 2013; Published online 3 July 2013
DOI: 10.1002/app.39416

INTRODUCTION

Polyethylene (PE) has excellent chemical and thermal stability, good mechanical properties, and a low price, and it is currently the most widely used polymer membrane material.[1] However, its hydrophobic properties are considered to be the key factor limiting the application of PE membranes, especially for water treatment.[2,3] First, the hydrophobicity of the membrane would cause high energy consumption during its use because a higher pressure would be required for water to penetrate the membrane. Second, the hydrophobicity could easily cause membrane fouling and lead to the rapid decay of the flux. Thus, hydrophilic modification is an important direction for high-performance PE membranes. Lots of effort has been put forth to improve the hydrophilicity of membranes; these have included as surface coating,[4,5] chemical grafting,[6,7] blending,[8–10] and plasma treatment.[11,12] Among them, the blending method is a convenient and effective method for surface modification.[13] The membranes modified by the blending method can not only avoid the disadvantages of the original component but also present some new features.

An important consideration for the blending method is the choice of the modifier. Extensive studies have focused on amphiphilic copolymers[14,15] because the hydrophobic segments usually have good compatibility with the matrix and can act as anchors in the membrane matrix to prevent the loss of the copolymer during the membrane preparation and operation processes. Meanwhile, the hydrophilic moiety always enriches the surface of the membrane, giving the membrane improved hydrophilicity.[16] In this respect, the maximization of the surface enrichment would have extremely vital significance. Generally, the content of the hydrophilic segments in the surface layer is regulated by changes in the dosing amount of the amphiphilic copolymer.[17,18] Even so, there are two drawbacks. First, the addition of too much copolymer would absolutely lead to a higher membrane cost. Second, the adopted copolymer usually has a relatively low molecular weight, which might cause unacceptable reduction in the mechanical strength of the blend membranes.[19] Hester et al.[20] reported that the temperature of the coagulation bath obviously affects the surface-enrichment behavior of the hydrophilic moieties in the nonsolvent-induced phase-separation process. This result indicates that the preparation conditions could also influence the surface chemical composition of the blend membranes. When the addition amount is fixed, the optimization of the surface modification could be achieved by the choice of suitable preparation conditions. However, few studies have been reported on the relationship between the preparation conditions of the thermally induced phase

Table I. Compositions of the Casting Solutions for Preparing the Membranes

Membrane code	HDPE/PE-*b*-PEG/LP (w/w)
M0	30/0/70
M1	27/3/70
M2	24/6/70
M3	21/9/70

separation (TIPS) process and the surface compositions of the obtained blend membranes.

PE-*b*-poly(ethylene glycol) (PEG) has been used to modify PE membranes via the TIPS process and has been proven to effectively enhance the membrane hydrophilicity and water flux.[3,21] The advantage of the TIPS method is that the preparation and modification can be achieved simultaneously. In this study, we explored the effect of the extractant on the surface composition in the preparation of high-density polyethylene (HDPE)/PE-*b*-PEG blend membranes via the TIPS process. Furthermore, in previous studies, diphenyl ether (DPE) was used as the diluent; it is not suitable for application in industry. In this study, environmentally friendly liquid paraffin (LP) was chosen as the diluent, and the preparation and performance of the HDPE/PE-*b*-PEG blend membrane were investigated.

EXPERIMENTAL

Materials

HDPE (5200B, weight-average molecular weight = 3.68×10^5) was provided by Lanzhou Petrochemical Co., Ltd. (China). PE-*b*-PEG (50 wt % PEG, number-average molecular weight = 1400) was purchased from Aldrich. LP, *n*-hexane, and ethanol were all provided by Shanghai Chemical Reagents Co. (China).

Phase-Separation Behavior of the Casting Solution System

Portions of HDPE, PE-*b*-PEG, and LP (Table I) were added to a flask equipped with a stirrer. The mixture was stirred into a homogeneous solution at 180°C, and it was then quenched by liquid nitrogen to yield solid HDPE/PE-*b*-PEG/LP mixture samples for phase diagram determination and membrane preparation. The obtained solid sample (ca. 10 mg) was placed between a pair of microscope cover slips and was heated on a hot stage (Linkam, THMS600, United Kingdom) at 180°C for 2 min and then cooled to 20°C at 10°C./min. The cloud-point temperature and the dynamic crystallization temperature (T_c) were determined visually by observation of the appearance of turbidity and crystallization of the polymer under an optical microscope (Nikon, Eclipse E600POL, Japan). The phase-separation behaviors of HDPE/LP were determined to be the same as those of the HDPE/PE-*b*-PEG/LP system.

Preparation of the HDPE/PE-*b*-PEG Blend Membranes

The casting solution and corresponding solid sample were prepared by the same manner as those in the previous section. The small pieces of the HDPE/PE-*b*-PEG/LP solid sample were put into a cube mold (thickness = 200 μm)[3] and thoroughly melted at 180°C. Then, the casting solution was compressed into a thin liquid film. The liquid film sandwiched in the template was quenched in a water bath (at 15°C) for 10 min, and the solid film (called the *precursor film*) was formed. The diluent LP in the precursor film was extracted by a specific extractant (ethanol or *n*-hexane) for 24 h at 25°C. The resulting porous membranes (coded as M0, M1, M2, and M3) were dried for 12 h in a vacuum oven at 30°C before characterization.

Characterization of the Membranes

The membrane structure was observed with a field emission scanning electron microscope (Hitachi S4800, Japan). The surface pore size was evaluated from the scanning electron microscopy images by Image Pro Plus software. The porosity (P) was calculated with the following equation:

$$P(\%) = (1-\rho_m/\rho_p)\times 100 \quad (1)$$

where ρ_m and ρ_p are the densities of the porous membrane and membrane matrix, respectively.[22] The thermal behaviors of membranes were characterized with a differential scanning calorimeter (PerkinElmer Pyris-1 DSC). The samples (5–8 mg) were sealed in an aluminum pan, and differential scanning calorimetry (DSC) curves were recorded from 40 to 160°C at 10°C/min under an N_2 atmosphere. The crystallinity (X_c) was calculated with the following equation:

$$X_c(\%) = H_f/\Phi H_f^0 \times 100 \quad (2)$$

where H_f and H_f^0 are the fusion enthalpies of the blend membrane and HDPE with 100% crystallinity (273 J/g[23]), respectively, and Φ is the weight fraction of HDPE in the blend membrane. The chemical composition was investigated by X-ray photoelectron spectroscopy (XPS; PHI Co., PHI 5000C ESCA system). The contact angle was measured by a contact angle measurement system (Dataphysics, OCA20, Germany) at 25°C.

Static Bull Serum Albumin (BSA) Adsorption

The protein antifouling characteristics of the membranes were evaluated with BSA as a model sample. The membrane was cut into a square, which had an external surface area of 8 cm^2. BSA solutions with various concentrations were prepared by the dissolution of BSA in a phosphate buffer solution (pH = 7.4). Then, the prepared samples were immersed in 10 mL of BSA solution at 30°C for 12 h and shaken at a speed of 150 rpm. The protein adsorption was determined as the different values of the concentrations of the BSA solution before and after the adsorption test divided by the surface area. The concentration was indicated by the UV absorption intensity at 280 nm, which was determined on an ultraviolet–visible spectrophotometer (Shimadzu, UV-1601, Japan).

Water Flux

The water flux was determined on a homemade device with a pressurized stirred test cell. The effective area was 12 cm^2. The samples were stabilized at 0.15 MPa with deionized water for about 0.5 h. Then, the test was performed under 0.1 MPa, and the flux was recorded when it was stable. The flux (J_w) is calculated by the following equation:

$$J_w = V/A\Delta t \quad (3)$$

where V is the volume of the percolating water, A is the effective membrane area, and Δt is the test time.

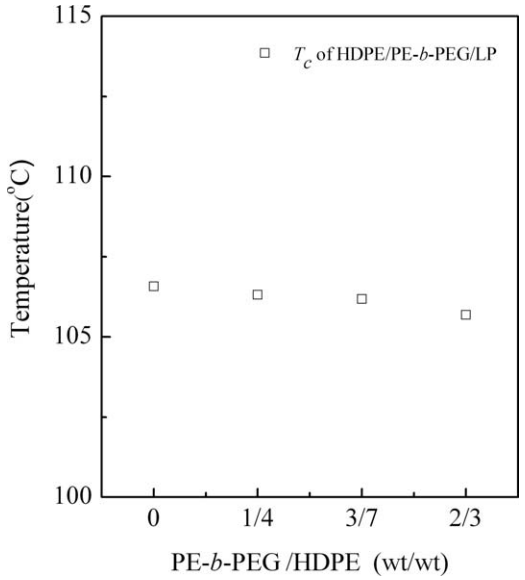

Figure 1. Phase diagrams of the casting solution system.

RESULTS AND DISCUSSION

Phase-separation Behavior of the Casting Solution System

Figure 1 shows the phase diagrams of the HDPE/PE-*b*-PEG/LP system in which total polymer concentration (HDPE and PE-*b*-PEG) was fixed at 30 wt %. In all of the investigated cases, only solid–liquid phase-separation occurred. This was because the solubility parameter (δ) of LP was 16.4 $(J/cm^3)^{1/2}$; this was close to that of HDPE [16.2 $(J/cm^3)^{1/2}$]. This indicated better interaction between HDPE and LP. When the thermal energy was removed, phase separation was induced by polymer crystallization. Furthermore, T_c decreased slightly (from 106 to 105°C) with increasing PE-*b*-PEG concentration in the casting solution. The reason was that with the total polymer concentration being fixed, the addition of PE-*b*-PEG led to a lower average molecular weight of the polymer and a lower viscosity of the system. This was beneficial for the movement of polymer segments, so polymer crystallization occurred at a lower temperature.

Compared to the pure HDPE/LP system, we found that the T_c of the HDPE/PE-*b*-PEG/LP system was slightly higher than that of the HDPE/LP system with same HDPE concentration. The reason was deemed to be the lower solution viscosity of the HDPE/LP system, which went against polymer crystallization. However, for all this, it is worth noting that the discrepancies caused by the existence of PE-*b*-PEG were very small.

Surface Chemical Composition

A typical TIPS process includes the preparation of the casting solution, a high-temperature melting process in the template, a cooling process to form the precursor film, an extraction process, and a drying process to obtain the final porous membrane. The extraction process could be regulated by a change in the extractant. Two completely different extractants (ethanol and *n*-hexane) were chosen. The discrepancies in the surface chemical compositions of the prepared membranes were investigated.

The surface composition was quantitatively characterized by XPS (Figure 2). The PE-*b*-PEG contents in the surface layer calculated on the basis of the XPS results are listed in Table II. For all of the prepared blend membranes, the PE-*b*-PEG content in the membrane surface was much higher than the corresponding theoretical value, no matter what kind of extractant was used; this indicated the enrichment of the PEG segments in the surface layer. This result was consistent with previous studies.[3,17] However, an interesting result was that the enrichment degree was obviously different when different kinds of extractants were used. When the nonpolar *n*-hexane was chosen as the extractant, many more PEG chains were enriched in the surface layer. As shown, when the dosage amount of PE-*b*-PEG was increased by three times (from 10 to 30%), the copolymer content on the surface only changed from 21.2 to 34.2 wt % when ethanol was

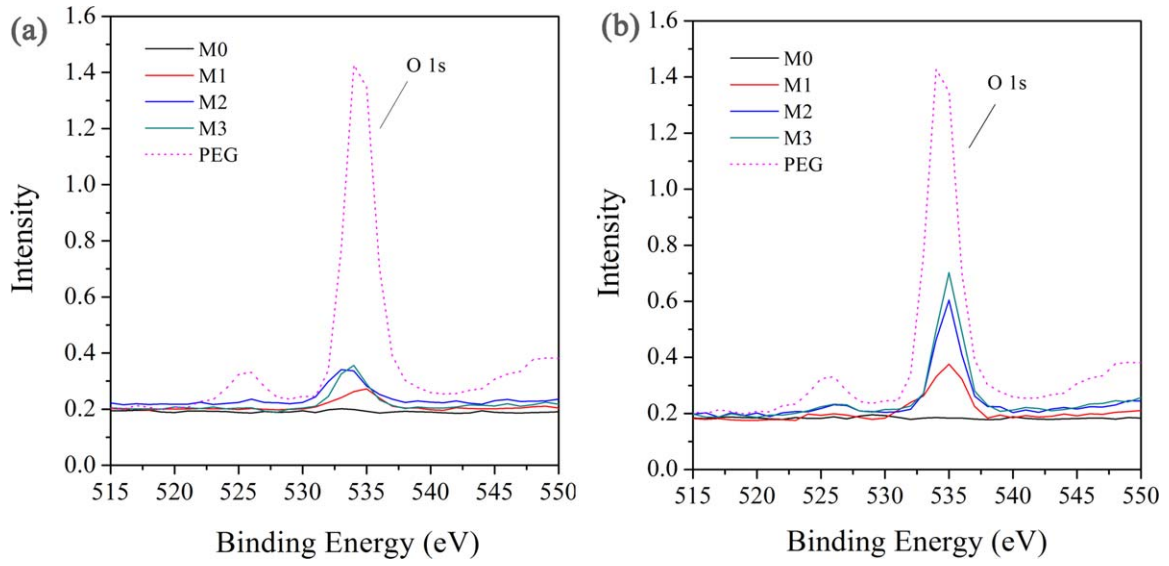

Figure 2. XPS results of prepared membranes extracted by (a) ethanol and (b) *n*-hexane (the value of the *y* axis was adjusted with the height of the C1s peak defined as 1). [Color figure can be viewed in the online issue, which is available at wileyonlinelibrary.com.]

Table II. Chemical Compositions of the Prepared Separators

Membrane ID	PE-*b*-PEG content in the whole membrane (wt %)[a]	PE-*b*-PEG content in the surface layer (wt %)[b]		Enrichment ratio	
		Extracted by ethanol	Extracted by *n*-hexane	Extracted by ethanol	Extracted by *n*-hexane
M0	0.0	—	—	—	—
M1	10.0	21.2	55.4	2.1	5.5
M2	20.0	28.0	80.4	1.4	4.0
M3	30.0	34.2	100.0	1.1	3.3

[a] Added to the casting solution.
[b] Calculated from XPS measurements.

used as the extractant, whereas the PE-*b*-PEG content in the surface layer could be elevated by two to three times when the extractant was changed from ethanol to *n*-hexane. The results suggest that the surface enrichment behavior could be effectively regulated by the choice of the extractant, which was more effective than the adjustment of the content of the additive.

The enrichment ratio is defined as the ratio of the PE-*b*-PEG content in the surface layer to the theoretical value. A high enrichment ratio indicates that the difference between the surface PE-*b*-PEG content and the amount of PE-*b*-PEG in membrane matrix is much larger; for example, many more PEG chains migrate onto the surface in the TIPS process. The enrichment ratio reached 5.5 for M1 with *n*-hexane as the extractant, whereas when polar ethanol was used, the enrichment ratio was only 2.1. All of the results suggest that the nonpolar extractant *n*-hexane was more favorable for the enrichment of PEG chains. In previous reports, the enrichment of PEG chains was deemed to be originally formed in the high-temperature melting processing in the template and the cooling process.[3,24] Because other preparation conditions were equal, the discrepancy of the enrichment degree in this study should have been caused in the extraction process. To explore the reason for the extractant effect, the δ and surface energy values of HDPE, LP, and PEG and extractant were compared and are listed in Table III. The solubility parameter for nonpolar *n*-hexane [$\delta_{n\text{-hexane}} = 14.6$ $(J/cm^3)^{1/2}$] was near to the solubility parameter of nonpolar HDPE [$\delta_{HDPE} = 16.96$ $(J/cm^3)^{1/2}$]. So, the HDPE matrix of the prepared membranes could be swollen by the nonpolar *n*-hexane,[25] and this could enhance the mobility of polymer segments. Meanwhile, low-molecular-weight PE-*b*-PEG chains embedded in the amorphous area of HDPE could be dissolved into the extractant and showed enough migration ability; this was further proven by DSC determination, as discussed in the following section. Thermodynamically, the dissolved PE-*b*-PEG chains also tended to diffuse from the center of the membrane to the surface and the extractant bath, which was all driven by entropy. Furthermore, from a comparison of the surface energies of HDPE, LP, and the extractants, we concluded that the surface energy of the precursor film was obviously higher than that of the extractants. This means that in the interface layer between the precursor film and the extractant bath, the PEG blocks tended to migrate into the precursor film rather than to diffuse into the extractant bath because of the characteristics of the amphiphilic block copolymer, for example, the decrease of the interfacial energy. Obviously, these two kinds of forces from the entropy drive and interfacial energy were in opposite directions. However, the enhanced surface enrichment suggested that the entropy and swelling effects dominated the interfacial energy effects. The reason might have been that in the extraction process, the real interfacial layer was not the layer between the pure HDPE and pure *n*-hexane. LP existed in the precursor film and in the *n*-hexane; this could have effectively decreased the interfacial energy effect. So, under the combined actions of the entropy drive and interfacial energy, the surface enrichment of the copolymer was further enhanced, although the membrane matrix could not be swollen by polar ethanol [$\delta_{Ethanol} = 25.8$ $(J/cm^3)^{1/2}$] and the motion of PE-*b*-PEG chains was prohibited. Finally, this caused a totally different surface enrichment amount for blend membranes with the same copolymer dosages.

Table III. δ Values and Surface Energies for HDPE, PEG, LP, *n*-Hexane, and Ethanol

Material	HDPE	PEG	LP	*n*-hexane	Ethanol
δ $[(J/cm^3)^{1/2}]$	16.9	22.5	16.2	14.6	25.8
Surface energy (mN/m)	31.9	42.9	33	18.4	22

As we know, when more PEG chains aggregate in a membrane surface, a better modification effect will be obtained.[3,17] Table II shows that the PEG content in surface layer calculated on the basis of XPS was up to 50 wt % for M3 when *n*-hexane was chosen as extractant. This was beneficial for the preparation of high-performance PE membranes.

Thermal and Crystalline Properties

The thermal properties of the prepared membranes were studied via DSC measurements (Figure 3). In the DSC curves, the endothermic peaks at about 124 and 130°C corresponded to the melting of crystalline HDPE in the blend membranes extracted by ethanol and *n*-hexane, respectively. The differences in the melting temperature (T_m) might have been caused by the rearrangement of polymer chains in the extraction process. M2 and M3 extracted by ethanol showed melting peaks of crystalline PE

Applied Polymer SCIENCE

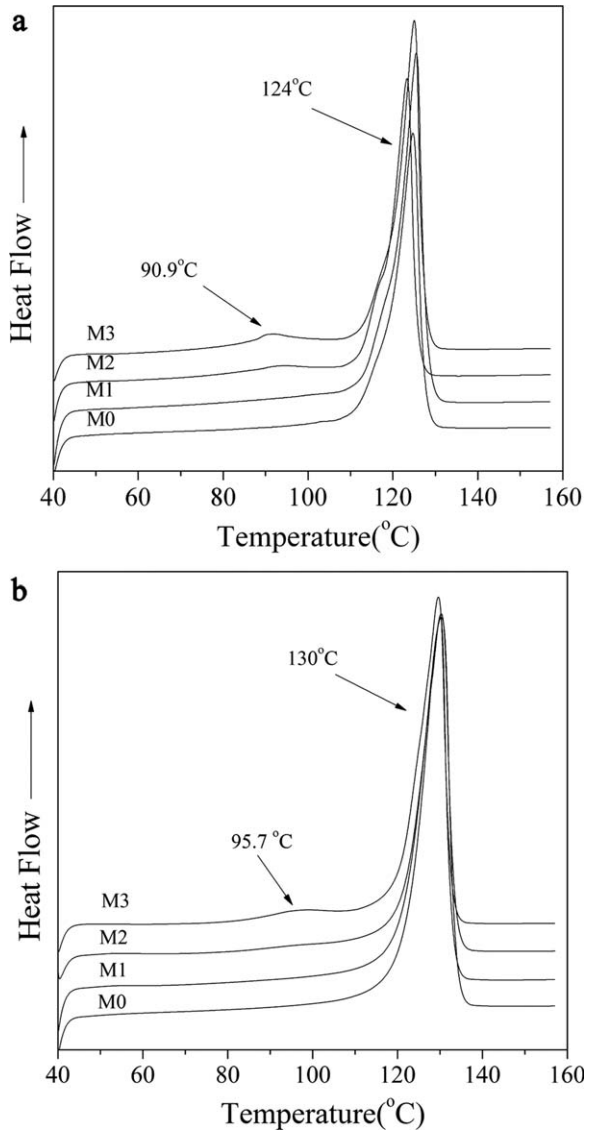

Figure 3. DSC curves of the membranes prepared with extracted by (a) ethanol and (b) *n*-hexane.

segments in the PE-*b*-PEG chains at 90.9°C, whereas M3 extracted by *n*-hexane showed a peak at 95.7°C. These results suggest that independent crystalline regions for the PE-*b*-PEG chains formed when the addition amount of the copolymer was increased to a certain degree.[24]

The crystallinities of the membrane, HDPE, and PE block in PE-*b*-PEG were calculated and are listed in Table IV. The crystallinity of the membranes extracted by ethanol decreased first and then increased. The reason was that the crystallinity of HDPE decreased first; meanwhile, the HDPE content in the blend membranes decreased because only the HDPE chains could crystallize when addition amount of PE-*b*-PEG was relatively low and the crystallinity of the whole membrane decreased. When the copolymer dosage was raised, the PE block in the copolymer also crystallized, as shown in Table IV, so the total crystallinity was also elevated. The crystallinities for the membranes extracted by *n*-hexane showed same trend. However, they were higher than for membranes extracted by ethanol. This was attributed to the increase in the HDPE crystallinity, which suggested that the rearrangement of chain segments and secondary crystallization occurred during the extraction process. Furthermore, the crystallinity of the PE block in the membranes extracted by *n*-hexane was lower than that in the membranes extracted by ethanol. The explanation might be that because the copolymer had a low molecular weight, the crystalline region could be easily swollen and even might have been totally dissolved by *n*-hexane,[21] and the copolymers tended to diffuse to the membrane surface rather than recrystallize because of entropy drive, so the crystallinity of the PE blocks decreased, although the crystal structure of the membrane extracted by ethanol might have changed little because ethanol could not effectively swell the membrane matrix. From this perspective, the effect of the extractant on the chemical composition and the crystallinity were in agreement.

Membrane Morphologies

Figure 4 shows the surface and cross-sectional morphologies of the prepared membranes. As shown, all of the membranes showed a similar pore structure on the surface and a similar spherulite structure in the cross section; this was caused by solid–liquid phase separation in the TIPS process. In a comparison of M0 and M3, the results suggest that the introduction of PE-*b*-PEG hardly influenced the membrane structure, in contrast to previous reports with DPE as the diluent.[3,17] The pore size tended to increase when the blend membranes were prepared by the HDPE/PE-*b*-PEG/DPE system. The reason was the different mechanism of pore formation. In the HDPE/PE-*b*-PEG/DPE system, because the dynamic T_c hardly varied, the pore size strongly depended on the liquid–liquid phase-separation temperature; this changed obviously when PE-*b*-PEG

Table IV. T_m and X_c Values of the Prepared Membranes

	Extracted by ethanol				Extracted by *n*-hexane			
		X_c (%)				X_c (%)		
Membrane ID	T_m (°C)	Membrane	HDPE	PE block	T_m (°C)	Membrane	HDPE	PE block
M0	124.7	52.7	52.7	—	130.0	63.8	63.8	—
M1	125.5	36.5	40.6	—	130.1	62.8	69.8	—
M2	123.3	38.4	47.5	7.5	130.3	56.3	70.4	0.0
M3	125.0	45.0	42.2	15.2	129.6	60.5	80.4	8.3

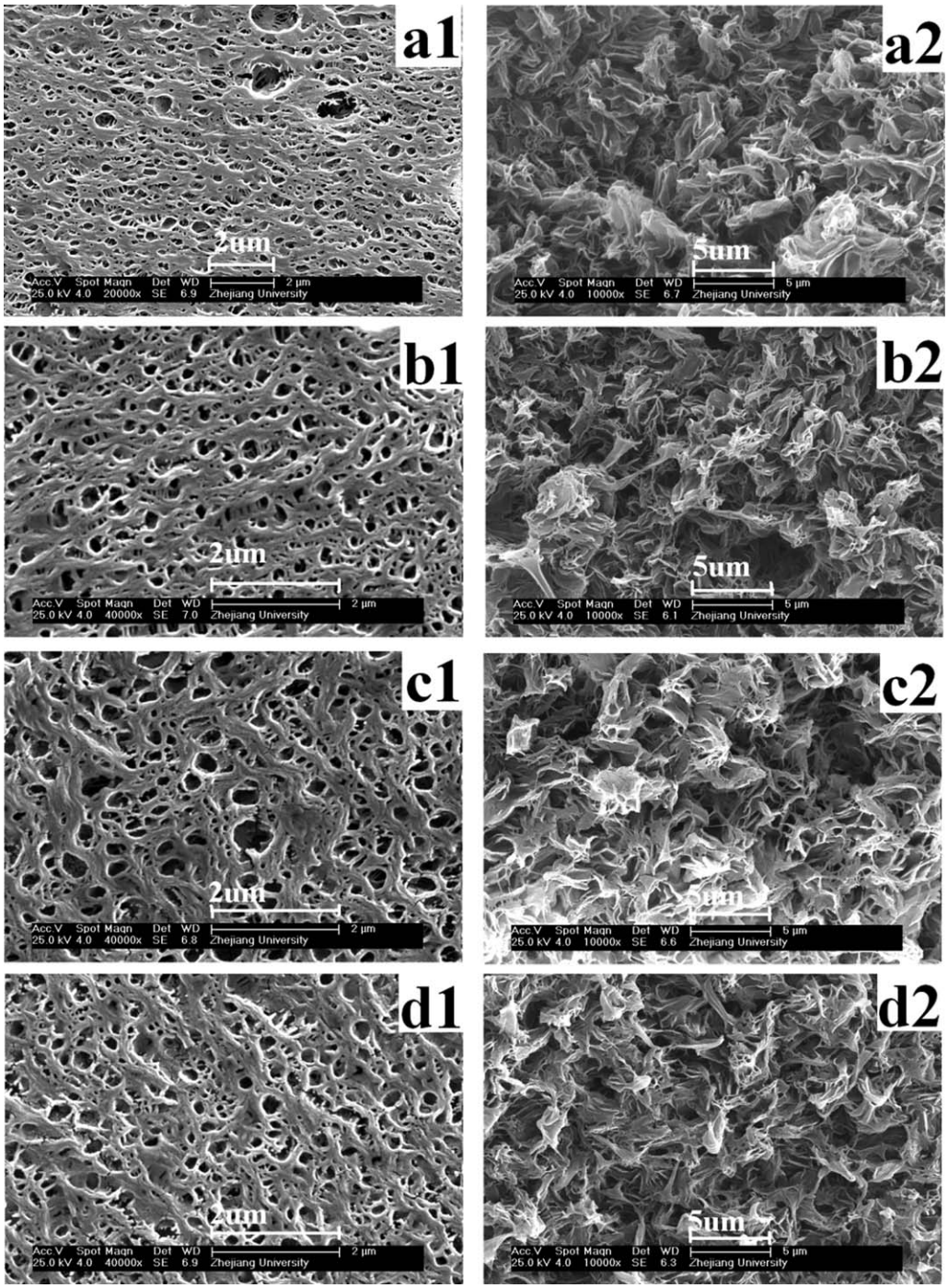

Figure 4. Surface (left) and cross-sectional (right) morphologies of membranes: (a) M0–*n*-hexane, (b) M3–*n*-hexane, (c) M0–ethanol, and (d) M3–ethanol.

was introduced.[26] In the HDPE/PE-*b*-PEG/LP system, the pore structure was induced by solid–liquid phase separation. However, the phase-separation behavior was less affected by the addition of PE-*b*-PEG, so the membrane structure and surface pore size (Table V) hardly changed. In theory, this kind of membrane structure should contribute to the penetration of water because of the existence of a more interconnected tunnel between the spherulites.[24] In addition, the extractants had no obvious effect on the membrane structures. This might have been because, although the swelling phenomenon existed, it only occurred in the surface layer of the surface and the pores rather than in the whole membrane matrix.

The porosities of the prepared membranes are shown in Table V; they changed little. This result was in accordance with the scanning electron microscopy results. In explanation, the pores were essentially the location for the diluent, so the porosity was mainly determined by the diluent content in the casting

Applied Polymer SCIENCE

Table V. Porosity and Pore Size Values of the Prepared Membranes

		Membrane code			
		M0	M1	M2	M3
Porosity (%)	*n*-Hexane	64.2	64.5	66.2	65.8
	Ethanol	65.3	63.1	65.9	67.3
Surface pore size (μm)	*n*-Hexane	0.43	—	—	0.40
	Ethanol	0.41	—	—	0.39

solution. Because the concentration of LP stayed same in this study, the porosity for all of the prepared membranes remained consistent. The similar membrane structures provided an experimental foundation for investigating the effects of the surface chemical composition on the membrane performance.

Membrane Hydrophilicity

The hydrophilicities of the membranes were evaluated by the contact angle and are given in Figure 5. As shown, the contact angle decreased effectively with the addition of the amphiphilic copolymer PE-*b*-PEG. M3 extracted by *n*-hexane showed the lowest contact angle of 64°, whereas the lowest contact angle of M3 extracted by ethanol reached about 96°. The improved hydrophilicity was attributed to the enhanced surface enrichment of the PEG chains. The results suggest that the hydrophilicities of the membranes could be effectively regulated by the control of the extraction process, especially through the choice of different kinds of extractants.

Membrane Performances

Figure 6 shows the BSA adsorption of membranes as a function of the BSA concentration. The adsorption was greatly depressed when more PE-*b*-PEG was introduced. M3 extracted by *n*-hexane had a BSA adsorption amount of 6.3 μm/cm^2 in 1.0 g/L BSA solution; this was far below that for M0 (36 μm/cm^2) under the same experimental conditions. Meanwhile, all of the adsorption values were lower than those for the membranes extracted by ethanol. It is well known that PEG chains possess exceptional resistance for the protein to contact with the membrane surface,[27] so when more PEG chains aggregate in the membrane surface, membranes would show an enhanced capability for reducing protein adsorption. That is, the enhanced surface enrichment of membranes extracted by *n*-hexane yielded membranes with better antifouling properties

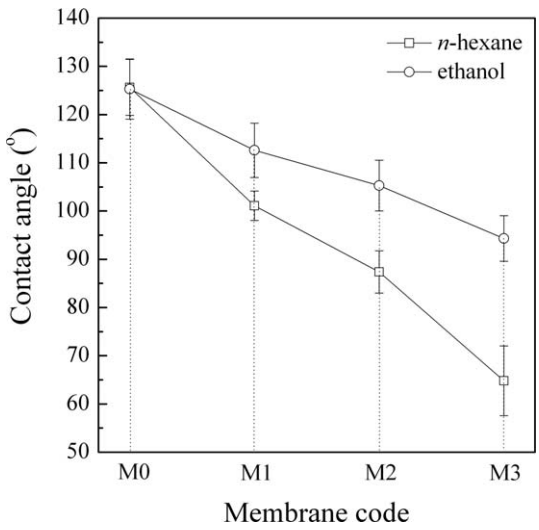

Figure 5. Contact angles of the prepared membranes.

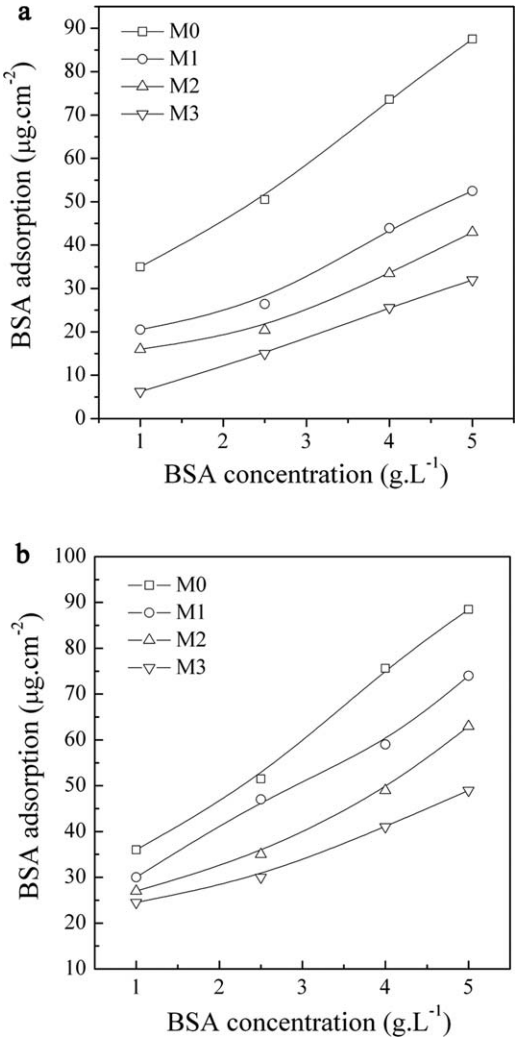

Figure 6. BSA adsorption of the prepared membranes extracted by (a) *n*-hexane and (b) ethanol.

The pure water permeation was determined at 0.1 MPa and is shown in Figure 7. The pure HDPE membrane extracted by *n*-hexane had a flux of 103 L m^{-1} h^{-1}; this was basically same as that of M0 extracted by ethanol. This was attributed to a similar membrane structure and porosity. In addition, the flux (of membranes extracted by *n*-hexane) increased dramatically when the addition amount of PE-*b*-PEG was elevated. For M3, the water flux reached 481 L m^{-1} h^{-1}. Meanwhile, the membranes extracted by ethanol showed same trend. However, the flux was much lower than that of the corresponding membranes extracted by *n*-hexane. Because all of the prepared membranes had basically the same structure, the changes in the flux were ascribed to the enhanced hydrophilicity.

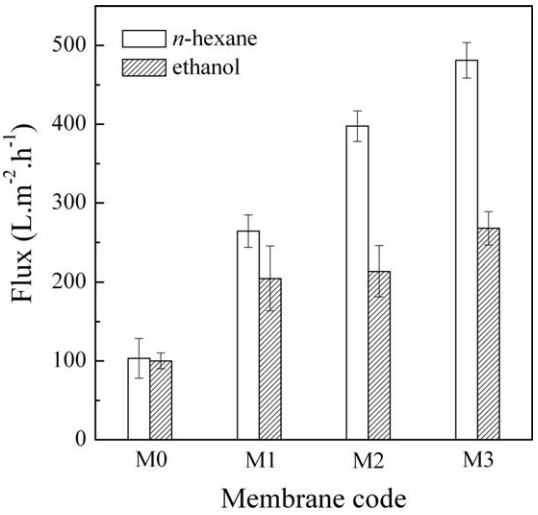

Figure 7. Water flux of the pure PE membrane and the blend membranes (pressure = 0.1 MPa).

Here, the flux was deemed to be dominated by two processes. First, the water infiltrated from the membrane surface into the pores. Second, the water flowed in the membrane pores. The first stage could be analyzed by the cylindrical capillary model.[28] The pores on membrane surface were regarded as the capillaries. According to the Laplace equation:

$$r_p = 2\gamma\cos\theta/\Delta P \quad (4)$$

where r_p is the pore size; γ and θ are the surface tension and the water contact angle, respectively; and ΔP is the difference between the external pressure and the internal pressure of the pore, which represents the critical pressure needed from the outside world to make the water to penetrate into the pores. When $\theta > 90°$, $\cos\theta < 0$. Because r_p and γ are positive, ΔP would be less than zero; this means that water penetration could not occur spontaneously. When θ is closer to 90°, $\cos\theta$ and ΔP tend to decrease to zero; this suggests that the critical pressure needed from the outside world would become smaller. Furthermore, when $\theta < 90°$, $\cos\theta > 0$ and $\Delta P > 0$; this indicates that the penetration behavior could take place spontaneously. The second stage, the water flowing in the pores, could be described by the Hagen–Poiseuille law.[28] In theory, the flow rate would be determined by the hydrophilicity of the wall of the pores because the pore size is small enough. However, once the pore wall is fully wetted and the flux test is performed at the same pressure, the difference in the flow rate should be very small.[28]

As reported by Vladisavljevic et al.,[28] for the hydrophilic membrane, the transmembrane pressure needed was zero because the water penetration could start autonomously. However, for the hydrophobic membranes, the critical pressure for water filtration was relatively high. For example, the critical transmembrane pressure needed for a membrane with a pore size 3.8 μm was reported as 30 kPa.[28] For the prepared membranes in this study, the hydrophilicity was enhanced with increasing PE-*b*-PEG dosage; this yielded a lower critical pressure or even a spontaneous force ($\Delta P > 0$) for water permeation at the first stage. When the membranes were subjected to the same pressure (0.1 MPa), the critical pressure decreased, and the remaining pressure for water flowing in the pores increased. So, the water flux tended to increase with increasing PEG chains on the surface.

CONCLUSIONS

HDPE/PE-*b*-PEG blend membranes were successfully prepared via a TIPS process. Environmentally friendly LP was used as the diluent. Only solid–liquid phase separation occurred in the membrane formation process, and this yielded membranes with a spherulite structure. The effect of the extractant was investigated. The results suggest that the nonpolar *n*-hexane was more conducive to the surface enrichment of the PEG chains than the polar ethanol; this was the result of the swelling effect combined with the entropy drive and interfacial energy effect. The modified membranes extracted by *n*-hexane showed enhanced hydrophilicity, antifouling properties, and flux. These results should contribute to a helpful understanding and technology in enhancing the properties of membranes in ways related to their chemical compositions.

ACKNOWLEDGMENTS

This work was financially supported by the Natural Science Foundation Committee (contract grant numbers 20974094 and U1134002) and National Key Basic Research and Development Program (973 Program) funded projects (contract grant number 2009CB623402).

REFERENCES

1. Matsuba, G.; Sakamoto, S.; Ogino, Y.; Nishida, K.; Kanaya, T. *Macromolecules* **2007**, *40*, 7270.
2. Gilron, J.; Belfer, S.; Väisänen, P.; Nystrom, M. *Desalination* **2001**, *140*, 167.
3. Zhang, C. F.; Bai, Y. X.; Sun, Y. P.; Gu, J.; Xu, Y. Y. *J. Membr. Sci.* **2010**, *365*, 216.
4. McCloskey, B. D.; Park, H. B.; Ju, H.; Rowe, B. W.; Miller, D. J.; Chun, B. J.; Kin, K.; Freeman, B. D. *Polymer* **2010**, *51*, 3472.
5. Chang, Q. B.; Zhou, J. E.; Wang, Y. Q.; Wang, J. M.; Meng, G. Y. *Desalination* **2010**, *262*, 110.
6. Liu, F.; Du, C. H.; Zhu, B. K.; Xu, Y. Y. *Polymer* **2007**, *48*, 2910.
7. Qiu, J. H.; Zhang, Y. W.; Shen, Y. B.; Zhang, Y. T.; Zhang, H. Q.; Liu, J. D. *Appl. Surf. Sci.* **2010**, *256*, 3274.
8. Qiu, Y. R.; Matsuyama, H.; Gao, G. Y.; Ou, Y. W.; Miao, C. *J. Membr. Sci.* **2009**, *338*, 128.
9. Rahimpour, A.; Madaeni, S. S. *J. Membr. Sci.* **2010**, *360*, 371.
10. Yi, Z.; Zhu, L. P.; Cheng, L.; Zhu, B. K.; Xu, Y. Y. *Polymer* **2012**, *53*, 350.
11. Steen, M. L.; Hymas, L.; Havey, E. D. *J. Membr. Sci.* **2001**, *188*, 97.

12. Kull, K. R.; Steen, M. L.; Fisher, E. R. *J. Membr. Sci.* **2005**, *246*, 203.

13. Rajabzadeh, S.; Liang, C.; Ohmukai, Y.; Maruyama, T.; Matsuyama, H. *J. Membr. Sci.* **2012**, *189*, 423.

14. Moriya, K.; Shen, P.; Ohmukai, Y.; Maruyama, T.; Matsuyama, H. *J. Membr. Sci.* **2012**, 415–416,*712*.

15. Ran, F.; Nie, S. Q.; Zhao, W. F.; Li, J.; Su, B. H.; Sun, S. D.; Zhao, C. S. *Acta Biomater.* **2011**, *7*, 3370.

16. Chen, X. R.; Su, Y.; Shen, F.; Wan, Y. H. *J. Membr. Sci.* **2011**, *384*, 44.

17. Liu, D.; Liao, H. Y.; Tan, N.; Xiao, G. Y.; Yan, D. Y. *J. Membr. Sci.* **2011**, *372*, 125.

18. Wang, J. L.; Liao, J. B.; Yang, L.; Zhang, S. G.; Huang, X. L.; Ji, J. B. *J. Membr. Sci.* **2012**, 415–416,*644*.

19. Tian, Z.; Pu, W. H.; He, X. M.; Wan, C. R.; Jiang, C. Y. *Electrochim. Acta* **2007**, *52*, 3199.

20. Hester, J. F.; Banerjee, P.; Mayes, A. M. *Macromolecules* **1999**, *32*, 1643.

21. Zhang, M.; Zhang, C. F.; Yao, Z. K.; Shi, J. L.; Zhu, B. K.; Xu, Y. Y.Chin. J. *Polym. Sci.* **2010**, *28*, 337.

22. Zhang, H.; Zhou, J.; Zhang, X. L.; Wang, H. T.; Zhong, W.; Du, Q. G. *Eur. Polym. J.* **2008**, *44*, 1095.

23. Gao, J. G.; Yu, M. S.; Li, Z. T. *Eur. Polym. J.* **2004**, *44*, 1533.

24. Shi, J. L.; Fang, L. F.; Li, H.; Liang, Z. Y.; Zhu, B. K.; Zhu, L. P. *J. Membr. Sci.* **2013**, *429*, 355.

25. Liu, Q. L.; Qian, W. *Polym. Mater. Sci. Eng.* **2005**, *21*, 153.

26. Shi, J. L.; Li, H.; Fang, L. F.; Liang, Z. Y.; Zhu, B. K.Chin. J. *Polym. Sci.* **2013**, *2*, 309.

27. Kang, S.; Asatekin, A.; Mayes, A. M.; Elimelech, M. *J. Membr. Sci.* **2007**, *296*, 42.

28. Vladisavljevic, G. T.; Shimizu, M.; Nakashima, T. *J. Membr. Sci.* **2005**, *250*, 69.